Evolution of a landslide-induced sediment wave in the Navarro River, California

Diane G. Sutherland*
Maria Hansler Ball
Susan J. Hilton
Thomas E. Lisle
USDA Forest Service, Pacific Southwest Research Station, 1700 Bayview Drive, Arcata, California 95521, USA

ABSTRACT

A streamside landslide delivered 60 000 m^3 of mixed-size sediment to the Navarro River, a sinuous gravel-bed channel (drainage area = 535 km^2), at the end of the annual high-runoff period in spring 1995. The deposit formed a 9-m-high dam that partially breached within several hours, but recessional flows entrained little material until the following high-runoff season. The landslide afforded the opportunity to measure the evolution of a sediment wave from its inception to near-obliteration and, particularly, to test relative tendencies for translation and dispersion of a sediment wave in a natural gravel-bed channel. This study represents a simple case: The wave originated from a single input, the preexisting channel was relatively uniform, and resistant banks prevented adjustments in width. We surveyed channel topography over a 1.5–4.5 km reach centered on the landslide dam each year from 1995 to 1999, and we sampled bed material downstream of the dam in 1995 and 1997. Landslide material was coarser than ambient bed material, but all sizes were mobilized by subsequent peak flows. Abrasion of weathered and fractured graywacke sandstone landslide material was roughly an order of magnitude greater than the ambient river gravel.

The sediment wave dispersed and mostly disappeared within a few years with no measurable translation. Sediment filled the reservoir created by the eroding landslide dam until throughput of bed load was restored in 1998. The stationary wave crest eroded until in 1999 it was <1 m higher than the preslide elevation. As the wave profile flattened, its detectable leading edge extended downstream from 620 m in 1995 to ~1600 m in 1997. Downstream advance of the wave was associated with coarsening of bed material.

The sediment wave created a longitudinal disturbance in sediment transport. By using the dam as a reference datum of zero bed-load transport, we computed longitudinal variations in annual bed-load and suspended-sediment transport rates in 100 m increments downstream of the dam. These longitudinal variations were controlled by scour and fill of the bed and by abrasion of bed-load particles. Bed-load transport rates in the first and second years after the landslide increased in the landslide vicinity and then decreased downstream as sediment deposited behind the advancing leading edge of the wave. The location of peak bed-load transport rate advanced from the first year (400 m) to the second (800 m).

We used a physically based, one-dimensional model (Cui et al., 2002b) to hindcast annual changes in transversely averaged bed elevation over the study reach. Agreement between measured and predicted bed elevations was very good. This result supports our conclusion that, once emplaced, sediment waves in gravel-bed rivers tend to disperse, with little or no translation.

Keywords: bed-load waves, geomorphology, modelling, sediment transport.

INTRODUCTION

Understanding the movement of sediment through channel systems is important to many geomorphic problems. In the short term (10^0–10^1 yr), sediment commonly carries the signature of upstream disturbances in runoff and erosion to downstream channels and valley bottoms and their aquatic and riparian ecosystems. The arrival, duration, and intensity of sediment impacts depend strongly on how excess sediment is distributed and interacts with stored sediment once it reaches the channel system. At longer time scales (10^1–10^3 yr), sediment fluxes build and modify alluvial landforms.

Sediment loads in channels are commonly punctuated in time and space by large inputs that produce sediment ''pulses'' or ''waves.'' Sediment waves are transient zones of sediment accumulation in channels that evolve by interactions between flow and sediment transport in the particular valley-bottom and channel topography through which they propagate. We adopt the term ''wave'' to refer to a propagating disturbance in bed elevation and sediment properties that might translate and/or disperse. Thus, a wave does not necessarily consist of only the original sediment of the input, but can also incorporate and mix with preexisting sediment in the river. The problem can be stated rhetorically: How do river systems digest large sediment inputs (Cui et al., 2002a)? Understanding how single sediment waves disperse and propagate should improve understanding of the routing of sediment from inputs distributed in a drainage network and thereby aid analyses of cumulative watershed effects. Such understanding should also improve predictions of the fate of large volumes of sediment released from decommissioned dams. In this study, we focus on a wave of bed material (sand and gravel) and neglect sediment transported in suspension.

A basic issue of the behavior of bed-material waves and their effect on stream channels

*E-mail: dsutherl@fs.fed.us.

GSA Bulletin; August 2002; v. 114; no. 8; p. 1036-1048 13 figures; 1 table.

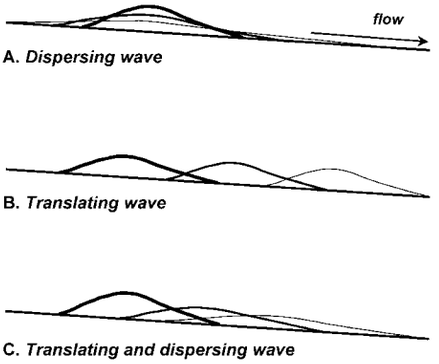

Figure 1. Models of sediment-wave evolution. Lighter lines symbolize later stages of evolution. (A) Sediment that is advected from upstream and incorporated in the wave is apparent in the dispersing wave as deposition upstream of the original wave. (B and C) In either of the translational cases, deposition immediately upstream of the input point is not apparent.

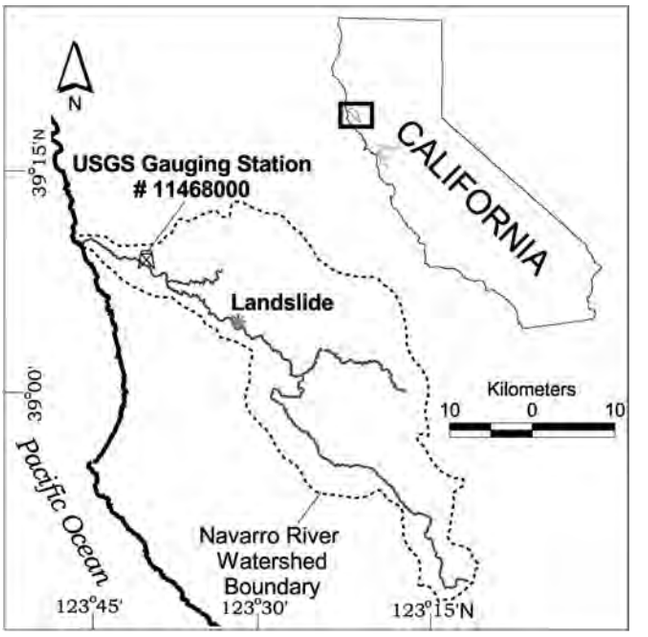

Figure 2. Location of study site.

is the relative tendencies for translation or dispersion. For purposes of discussion, a purely dispersive wave is one whose trailing edge and apex do not migrate downstream, although its center of mass may shift as its front advances (Fig. 1A). The backwater effect of the wave may cause sediment advected from upstream to accumulate on the upstream limb of the wave. The result is a more symmetric spread of the wave about its point of origin. In a translational wave, both leading and trailing edges and the wave apex advance downstream (Fig. 1B). A reasonable expectation is for a wave to both translate and disperse to various degrees (Fig. 1C). The relative strength of these tendencies is important for predicting sediment impacts. Dispersion of sediment inputs attenuates but prolongs impacts downstream, whereas translation preserves pronounced sequences of impact and recovery as the wave migrates downstream. In a natural channel, topography can force longitudinal variations in deposition, making degrees of dispersion and translation difficult to discern. Monitoring bed elevation with little knowledge of preexisting elevations at scattered points along the channel can lead to ambiguous interpretations of wave evolution, as noted by Lisle et al., 2001.

Expectations of wave behavior have been influenced by Gilbert's (1917) landmark study of sediment waves produced by hydraulic mining of placer deposits along tributaries of the American and Sacramento Rivers in California. His conclusions (p. 30) regarding wave behavior emphasize translation: ''The downstream movement of the great body of debris is thus analogous to the downstream movement of a great body of storm water, the apex of the flood traveling in the direction of the current.'' Results of a numerical model of Benda and Dunne (1997) predict translation and dispersion of sediment waves downstream of sediment sources in a basin in the Oregon Coast Range. Miller and Benda (2000) observed channel morphology and bed texture after a high-magnitude flood in a steep channel and interpreted their observations to indicate translation of a wave of debris-torrent material. However, other studies of sediment waves in rivers show strong dispersion and weak or questionable translation (Roberts and Church, 1986; Knighton, 1989; Pitlick, 1993; Turner, 1995; Madej and Ozaki, 1996). Recent numerical models and laboratory experiments indicate the dominance of dispersion in the evolution of sediment waves in gravel-bed channels (Lisle et al., 1997; Dodd, 1998; Lisle et al., 2001; Cui et al., 2002a, 2002b). Wave translation is enhanced by low Froude numbers (typical of low-gradient, sand-bed channels) and wave material that is finer than ambient streambed material (Meade, 1985; Lisle et al., 2001).

This paper reports detailed measurements of the evolution of a sediment wave in the Navarro River in north coastal California from its inception as a landslide through late stages of evolution. The results provide an unambiguous evaluation of the relative degrees of translation and dispersion of an evolving sediment wave in a natural channel. In this case, widely graded input sediment is coarser than the ambient river gravel, but all sizes are mobile. We relate field observations to theory by testing predictions of a one-dimensional numerical model of wave evolution (Cui et al., 2002b) that is based on first principles of conservation of water mass and momentum and sediment, but also includes empirical values based on field and laboratory data on gravel transport. Field and modeling results confirm that the wave is exclusively dispersive.

STUDY SITE AND LANDSLIDE EVENT

The Navarro River is located in north coastal California (Fig. 2) in a temperate maritime climate. Mean annual precipitation is ~130 cm, nearly all of which falls as rain from November to March. Vegetation consists of mixed hardwoods and conifers and prairie grasslands in the headwaters, vineyards and orchards in the upper main stem, and second-growth forests along the lower main stem. Local lithology is the Coastal Range terrane of the Franciscan Formation, chiefly composed of highly sheared sandstone and siltstone as well as some mudstone (Manson, 1984). Drainage area at the study reach is 535 km^2. A U.S. Geological Survey gauging station (#11468000; drainage area = 785 km^2) is located 25 km downstream of the study reach; it recorded an average 15-minute discharge of

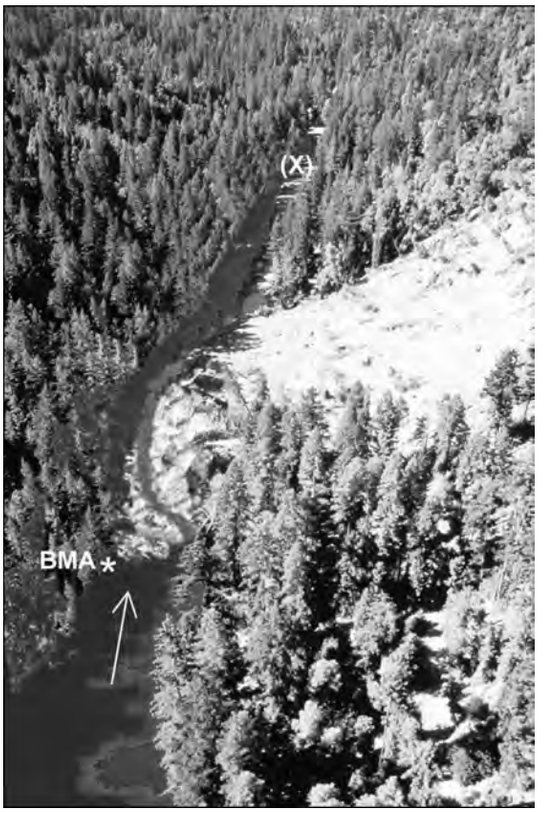

Figure 3. View looking downstream at the landslide entering the Navarro River, March 1995 (photograph provided by Julie Sowma-Bawcom, California Geological Survey). Arrow points to remnants of the landslide dam, which provides the zero bed-load transport datum. The sediment wave extended downstream to (X) in 1995. Asterisk indicates the approximate location of BMA.

14.5 $m^3 \cdot s^{-1}$ for the period of record (1950–2000). Bankfull width and depth at the study reach are ~57 m and 5.1 m, respectively; bankfull discharge ($Q_{2.33}$), calculated by prorating drainage area at the landslide site (68%) to the gauge, is 385 $m^3 \cdot s^{-1}$. Discharges with a recurrence interval of 2.33 yr correspond well with the depth at which we find many bankfull terraces.

On March 23, 1995, a translational-rotational landslide mobilized ~100 000 m^3 of soil and sheared and weathered bedrock and delivered 60 000 m^3 into a straight reach of the Navarro River (Fig. 3). The landslide occurred at the end of an extremely wet winter along a preexisting weakness in the rock (Sowma-Bawcom, 1996). Before the landslide, the hillslope supported a young forest of tan-oak (*Lithocarpus densiflorus*), mixed evergreens (primarily *Pseudotsuga menziesii*, *Quercus* spp., and *Arbutus menziesii*), *Ceanothus* spp., and redwood (*Sequoia sempervirens*). The landslide buried a 120-m-long reach of river to a depth of 9.3 m. Discharge (~130 $m^3 \cdot s^{-1}$) was subbankfull at the time, but the ponded flow overtopped the landslide dam and eroded a narrow channel over the next 12 h, transporting and depositing sand, angular gravel, and woody debris over ~620 m of channel downstream. Afterward, discharge waned rapidly and remained low until the next winter. The residual landslide dam, which contained a sparse framework of large woody debris, was 4.5 m high and created a pond that extended 2.2 km upstream of the slide. The pond (locally called Lake Navarro) filled with bed load over the course of the following 3 yr.

Landslide material consisted of mudstones, sandstones, siltstones, and minor volcanic lithologies. These rocks readily break along pervasive shear planes and abrade to fine sand and silt. Landslide debris was coarser than the preexisting bed material although sorting was similar (described later). Ambient gravel was composed of lithologies similar to those of the landslide but was more rounded and competent and included minor amounts of chert.

The study reach extends from 2.6 km upstream to 1.9 km downstream of the landslide. Active floodplains are narrow, and the channel is moderately confined alternately by valley walls and high (>5 m) terraces. Channel banks are stable, consisting mostly of either bedrock or densely rooted fine alluvium. Bank erosion during the study period was minimal despite local aggradation and the occurrence of some large floods. The channel has a relatively simple, single-thread, bar-pool morphology with an average channel width of 44 m, average pool spacing of 210 m (4.8 channel widths), and a gradient of 0.0013. Large roughness elements (e.g., large woody debris, outcrops, boulders) are uncommon, although willows grow on bars within the active bed.

In summary, this landslide provided a rare opportunity to measure the evolution of a wave of sediment in a natural channel. It was fortunate for this purpose that the wave was emplaced in a single event during waning stages of the high runoff season, which enabled us to measure initial stages of wave evolution in detail. Channel morphology was relatively simple, uniform, and characteristic of many gravel-bed rivers. Erosion-resistant banks eliminated channel widening as a significant adjustment to wave evolution. The input sediment was somewhat coarser than the ambient bed material, but all particles were transportable.

METHODS

Our strategy was to measure variations in channel topography and bed texture annually over the entire reach affected topographically by the sediment wave until the wave was mostly dissipated. Topographic data were transversely averaged and compared to predictions of a one-dimensional model (Cui et al., 2002b). We measured particle-size distributions of surface and subsurface bed material to investigate sorting of wave sediment in relation to topographic changes. We experimentally measured abrasion rates of landslide material and ambient river gravel in order to measure the contribution of particle abrasion to downstream fining and sediment-wave evolution. We used topographic data and abrasion rates to analyze longitudinal variations in transport rates. In the following sections, we describe our methodology in detail.

Topographic Surveys

During the course of the investigation, the wave crest remained at the landslide dam and logically divided the wave into an upstream

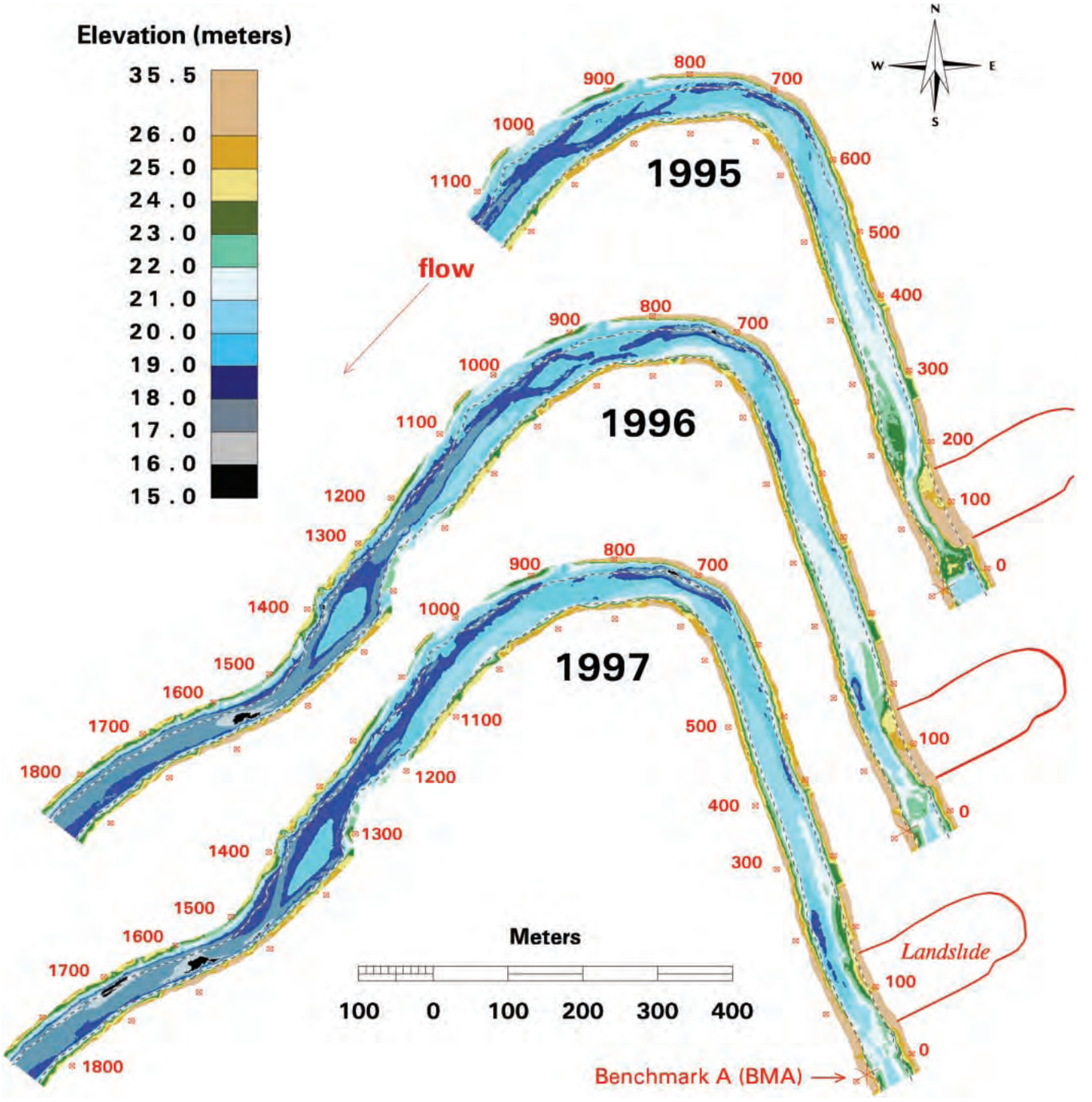

Figure 4. Channel topography of the downstream limb of the sediment wave. Numbers in red are longitudinal distances (in meters) from BMA. Dashed lines indicate edges of active bed used in calculating year-to-year change in bed elevation (meters above mean sea level), and dashed red and black lines indicate edge of active bed through the landslide each year.

limb measured as negative distances from bench mark A (BMA) at the upstream edge of the dam and a downstream limb measured as positive distances from BMA. In the first year, topographic surveys of the study reach extended from −300 m to 1200 m. The next year, the study reach was expanded to ~2600 m upstream and downstream in anticipation of the spread of the sediment wave. We surveyed the channel in greatest detail from 0 to 1200 m in 1995 and from 0 to 1860 m in 1996 and 1997. From this we generated digital elevation models (DEMs) having a 1 m cell size. We used cross-sectional surveys to expand coverage upstream and downstream in less detail

in 1995–1997 and to measure elevations in the entire study reach in 1998 and 1999. In the intensively surveyed reach, we used a total station electronic surveying instrument and a ranging-laser with internal compass to survey bed elevations in closely spaced (<5 m), loosely gridded intervals. Point coverages, which are two-dimensional, computer-generated representations of geographic data sets, were produced from Cartesian coordinate survey points. Point coverages were transformed to triangulated irregular networks (TINs) by connecting nearest-neighbor survey points as vertices to create a triangular surface network and, finally, a 1 m (horizontal dimension) DEM (Hansler, 1999). We estimated survey error by comparing DEMs to independently surveyed cross sections at the same locations. The absolute value of the mean difference in elevation between a DEM point and a survey point was 0.04 m (±0.11 m) (Hansler, 1999). The fact that this value was no greater than the characteristic particle roughness of the bed in the vicinity of the landslide (D_{84} = 0.10 m) validates a detailed examination of two-dimensional variations in bed elevation. Error for transversely averaged bed elevations was even less (0.004 m) because of the large sample size. These estimates of error apply equally to cross-section surveys.

Longitudinal profiles of transversely averaged bed elevations were generated by projecting elevations from the 1 m DEM grid onto a midchannel line that was generated from the midpoint of the shortest distance between lines defining left and right edges of the active channel bed. Mean bed elevations were computed as the average of all points in a 20 m interval and were plotted at the interval's midpoint. The profiles we constructed by using the entire bed represent more area on the outside of a bend than on the inside. Longitudinal profiles computed in this way will differ from profiles constructed by using cross sections, which weight the outside and inside of a bend equally. There is one major bend in the study reach, and we consider it to be insignificant to the interpretation of our results.

Particle-Size Distributions of Bed Material

Exposure of most of the bed during the annual summer drought greatly facilitated bed-material sampling. We mapped and measured surface particle-size distributions from +200 m to the downstream end of the intensively surveyed study reach in 1995–1997. We delineated patches of like particle-size distributions that were categorized into unimodal distributions of (1) sand and fine gravel, (2) medium gravel, or (3) coarse gravel or very poorly sorted or bimodal distributions of (4) fine or (5) coarse gravel. We conducted pebble counts (Wolman, 1954) of no less than 100 particles on a subsample of randomly selected patches of each distribution type in 1995 (31% by number) and 1996 (24%) and on every patch in 1997. We averaged surface particle-size distributions over 50-m-long channel segments to investigate longitudinal variations in particle size and sorting. Pebble counts were recorded in half-ϕ intervals to −2ϕ (4 mm), and smaller particles were combined into a <4 mm category.

In the same reach, we collected 13 bulk samples of subsurface bed material in 1995 and 10 in 1997. In 1995, we selected sample locations at random *x*-, *y*-coordinates to equally represent each patch type by area covering the entire study reach. In 1997, we extracted one subsurface sample in each 200-m-long channel segment downstream of the landslide. Correlations between surface and subsurface particle-size distributions at the patch scale (Mosley and Tindale, 1985; Lisle and Madej, 1992; Buffington and Montgomery, 1999) led to the approximation that the reach-averaged subsurface size distribution can be found under patches whose bed surface size distributions equal the reach-averaged bed surface size distribution (Lisle and Madej, 1992). By using visual estimation and referring to sample pebble-count data, we approximated the average surface particle-size distribution for each segment, found a location on the bed that corresponded to the average surface distribution, and sampled there. We used averages of four 1995 bed-material pits immediately downstream of the landslide to represent the particle-size distribution of the initially deposited sediment-wave material. We sampled bed material downstream of the sediment wave in 1995 to represent the ambient bed-material distribution.

We extracted subsurface samples after removing the surface layer to a depth equal to D_{90}. We air-dried and sieved samples at half-ϕ increments on-site, except for a subsample of <11.2 mm material that we sieved later in a laboratory down to a minimum sieve size of 0.5 mm, which we assumed was the upper limit of sizes that could be suspended. Individual subsurface samples ranged from 100 to 425 kg. In most cases, this range met the criterion of Church et al. (1987) that the largest particle in the sample has a mass of <1% of the total. However, near the sediment-input source, the presence of boulders required us to accept a 5% limit (Mosley and Tindale, 1985).

Abrasion Rate

Breakdown and abrasion of landslide particles were apparently rapid. In 1995, many landslide particles on the stream bed surface were broken into small fragments, apparently a result of the sand- and siltstone particles having disaggregated after being exposed to surface conditions. Downstream, gravel from the landslide could easily be distinguished from ambient river gravel by weathering coloration, angularity, and obvious fracture planes. In addition, while sampling bed material in 1995, we noticed that many of the particles were very friable and broke easily during the sieving process.

We used an abrasion mill in the form of a tractor tire to measure rates of abrasion of initially deposited sediment-wave material collected within 50 m downstream of the slide and ambient gravel collected upstream. In the abrasion tests, we ran samples over distances totaling 1000 m, which approximated the maximum apparent travel distance of landslide material. For each sample, we placed 25 kg of material with a representative size distribution (D < 180 mm) in a 1-m-diameter tractor tire, in which rubber vanes <1 cm in height were glued to promote particle rolling. We held the tire upright, filled it up to the lower lip of the rim with the sample and water, sealed the opening, and rolled the tire a specified distance at ~2 $m \cdot s^{-1}$. All material was then removed from the tire, air-dried, sieved to separate the <0.7 mm fraction, and reweighed. The same material minus the <0.7 mm fraction was reloaded into the tire and run for the next interval, and so on, until a total of 1000 m was traversed. Results of preliminary runs indicated that abrasion rates of the wave material varied with travel distance and were significantly affected by wetting-drying cycles, but such was not the case for ambient river gravel. Therefore, we ran wave material over 100 m intervals to replicate step distances and ran ambient gravel over longer intervals.

It is highly uncertain whether we accurately replicated natural abrasion rates on the river bed. We selected tire speed to approximate maximum bottom-water velocities, but particle motion in the tire can be expected to differ from that on the river bed. Nevertheless, our measured abrasion rates were reasonable considering the material (discussed later), and model predictions of sediment-wave evolution were not sensitive to moderate variations in input abrasion rates.

CHANNEL TOPOGRAPHY

Initial Topography, 1995

The intensive 1995 survey of the downstream limb of the wave (Fig. 4) documented a morphology created by the landslide and the dam-break flood; subsequent flows were too small to cause significant sediment transport until the 1995–1996 winter. The width of the channel that had incised through the landslide (channel distance from 30 to 150 m) was only 10 m, or about one-fourth that of the preexisting channel. Debris eroded from the breached landslide was deposited as a downstream-thinning wedge that could be detected by angularity and lithology as far as 620 m, just upstream of a major left bend in the channel, although a few landslide clasts were found as far as 900 m. The breach occurred on the left side of the channel, but the channel downstream was forced to the right by a large, wood-mantled bar (150–270 m) that was apparently deposited by a debris flow during late stages of the landslide event. The bar was as high as 2 m above the 1995 low-flow water surface and approximately twice as high as bars elsewhere. A pool at the landslide site and another at 250–300 m downstream that were evident on a 1993 aerial photograph were filled, but two new shallow troughs were created between new alternate bars from 400 to 600 m.

The longitudinal profile of mean bed elevation shows a downstream-thinning sediment wave with a maximum elevation (25.5 m above mean sea level) that was 4.5 m above the estimated prelandslide mean bed elevation and extended downstream to 620 m (Fig. 5). In 1995, Lake Navarro had a water surface elevation of 23.1 m and extended 2200 m upstream. A thin (0.1–0.5 m), fine-grained, low-density deposit blanketed the pond bed, and a sandy delta with an estimated thickness of 0.3–0.5 m prograded into Lake Navarro.

Water Year 1996

In water year 1996 (WY 1996; October 1, 1995, to September 30, 1996), the highest flow (259 cm·s) was less than the mean annual flood (Fig. 6), and its duration was only 4 h. Nevertheless, there was substantial evolution of the sediment wave. Erosion of the toe of the landslide increased channel width twofold (Fig. 4). The debris-flow bar at 150–270 m was eroded away, resulting in a 3.5-m-deep pool, and a sandy reattachment bar was deposited along the opposite bank in the lee of the landslide. More subtle changes downstream are revealed in a map of scour-and-fill depths (Fig. 7). Maximum changes in bed elevation occurred in the first 250 m. Alternate bars and pools in the straight reach downstream (300–600 m) shifted slightly. Farther downstream in the large bend and beyond, pools scoured as bars filled.

The 1996 longitudinal profile (Fig. 5) shows no translation of the wave in the first year. The apex remained at the toe of the landslide but lost 2.7 m in elevation. The 1995 and 1996 profiles crossed at ~500 m, and a short reach of fill (<0.4 m deep) extended downstream to 650 m, indicating a slight extension of the downstream limb of the wave. Beyond that, the change in mean bed elevation did not exceed 0.3 m. There was a net loss of 16 000 m^3 of sediment from the downstream limb. On the upstream limb, the lake level dropped 1.6 m, and lake length decreased by 1000 m. Sedimentation of mud, silt, sand, and fine gravel increased mean bed elevation immediately upstream of the dam as much as 0.8 m. From −1200 to −2000 m, sediment inundated alders, which commonly grow near summer-flow margins, indicating that the channel had aggraded ~0.5 m in WY 1996 compared to estimated preslide elevation.

Water Year 1997

Flows in the second winter of study (WY 1997) were larger than those of the first (Fig. 6). Four storm flows exceeded bankfull, in-

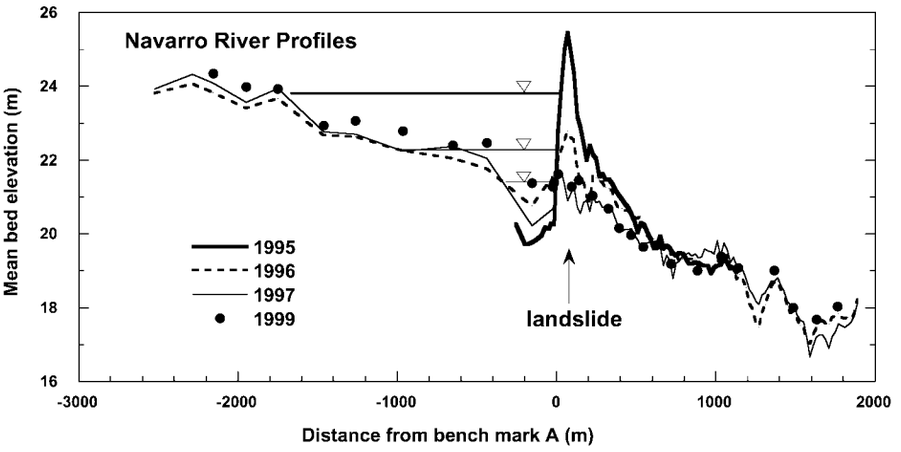

Figure 5. Longitudinal profiles of transversely averaged bed elevation (Sutherland et al., 1998).

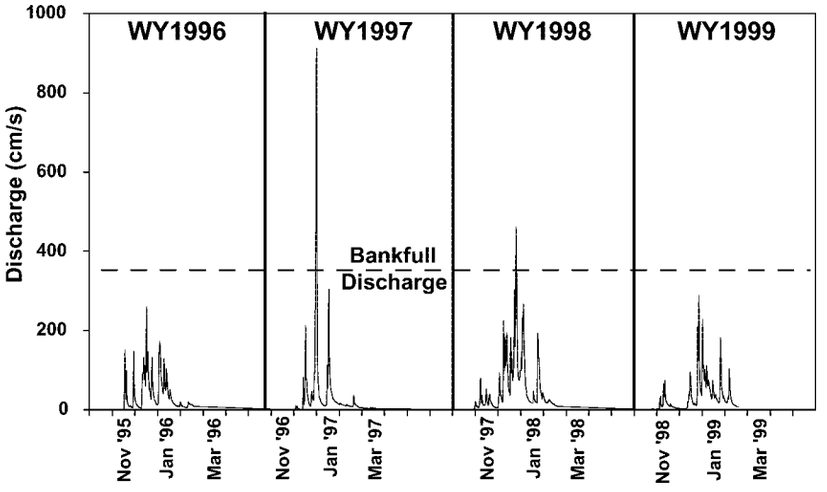

Figure 6. Annual hydrographs for the study site, October–April 1996–1999. Flow data from USGS gauging station #11468000 were adjusted by prorating discharge to the drainage area at the landslide (68% of the area at the gauge).

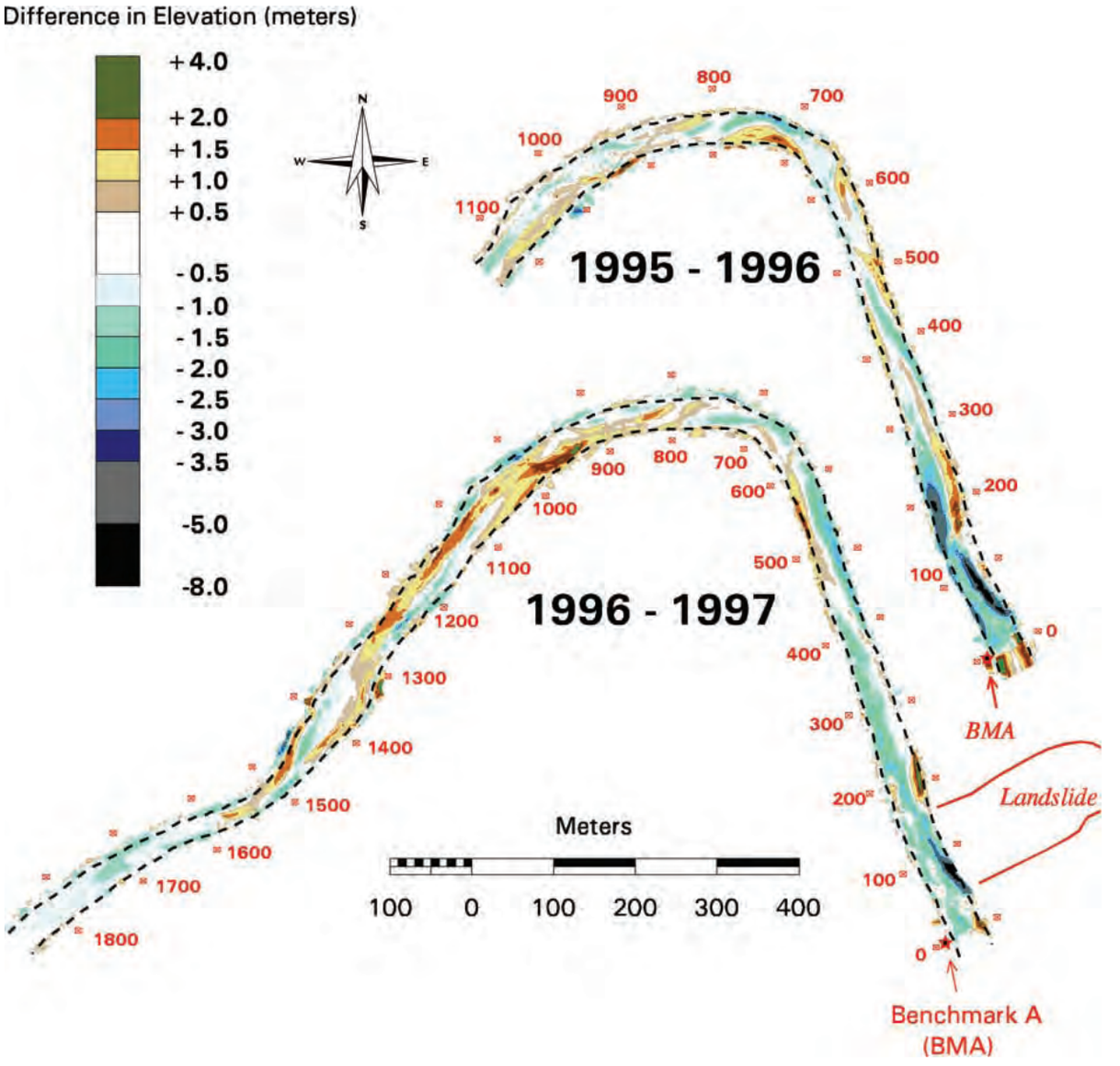

Figure 7. Depths of scour and fill in the downstream limb of the sediment wave.

cluding one that reached a peak 15-minute discharge of 1150 $m^3 \cdot s^{-1}$ (~7 times bankfull discharge) and sustained flows over bankfull for 12 h. In total, bankfull flow was exceeded for 36 h in WY 1997.

This high flow resulted in further substantial evolution of the sediment wave (Figs. 4 and 7). However, despite the greater flows of the second winter, net loss of material from the downstream limb (15 000 m^3) was approximately equal to that resulting from the first winter. The river continued to erode the landslide toe, regaining 80% of its preslide width. The sandy bar along the right bank at 200 m to 250 m aggraded >1 m. The left-bank alternate bar originating from the pool at 200 m elongated and buried the left-bank trough downstream at 500–600 m. Meanwhile, the right-bank trough adjacent to this bar (at 400–600 m) elongated into the bend. Little change occurred in the bend, but downstream there was substantial deposition at the head of the large, left-bank bar originating at ~900 m and in troughs (1000–1600 m) farther downstream.

Changes in the longitudinal profile in 1997 continued the trends of the previous year (Fig. 5). The apex of the wave was eroded another 1 m but remained in place (at 70 m). The channel downstream degraded a lesser amount (<0.5 m) to ~600 m and aggraded (0.2–0.5 m) from 800 to 1600 m. Downstream of 1600 m, the channel scoured ~0.5 m. The downstream limit of the wave is unclear. The advancing wedge can be discerned as far as 1000 m, but bar-pool topography obscures systematic changes in mean bed elevation farther downstream.

On the upstream limb, Lake Navarro dropped 0.9 m and receded another 400 m in length. Small deposits of well-rounded gravel (D_{50} = ~10 mm) were found downstream of the dam, indicating that some bed load passed through Lake Navarro and over the landslide dam. Cross sections from −175 m to 0 m showed scour of fine material that was deposited in WY 1995. Farther upstream to −2200 m, average cross-section elevation increased by ~0.1 m.

Water Years 1998 and 1999

Water years 1998 and 1999 had flood peaks greater than those of WY 1996 but not nearly as great as the large peak of WY 1997 (Fig. 6). Changes in the longitudinal profile were small from WY 1998 and hardly detectable from WY 1999 (Fig. 5). Changes in the downstream limb were minor, but slight aggradation can be detected near the end of the study reach (1800 m), suggesting farther advance of the wave. On the upstream limb, a slightly downstream-thickening wedge averaging ~0.5 m thick was deposited from −1500 to −15 m in WY 1998. The wave crest eroded an additional 0.5 m and, as a result, no longer ponded water.

The overall effect was to leave a broad hump in the profile over the entire study reach. By 1998, the wave had no clearly defined apex and had lost most of its topographic expression. The wave was primarily revealed by a transition from fine rounded gravel upstream of the landslide to coarse, subangular gravel downstream. Downstream of ~1500 m, the only evidence of the sediment wave was a few subrounded cobbles.

In summary, our surveys document most of the evolution of a sediment wave from inception to obliteration. Longitudinally, these changes indicate a sediment wave that is decaying in amplitude as sediment is accreted upstream and is spread downstream. After 4 yr, the wave evolved into a broad, low hump in the river profile and lost all obvious topographic expression within 2 km of the landslide. Its legacy was a discontinuity in bed texture created by the lag of landslide particles. We predict that the wave will disappear as lag particles break down further and mix with ambient bed load.

At a smaller scale, bed-elevation changes were manifested as deformation of bar-pool topography. On the upstream limb of the wave, backwater deposition of fine sediment from upstream tended to bury bar-pool topography. Downstream of the dam, large volumes of coarse landslide material obliterated preexisting bars and pools and formed new ones that later elongated. Farther downstream, bars and pools were preserved as the thinning sediment wedge extended. Bars were predominantly filled, whereas pools were either filled or scoured.

PARTICLE-SIZE DISTRIBUTIONS OF BED MATERIAL

The landslide material delivered to the channel was angular and very poorly sorted; the material comprised clay to a few boulders as large as 2 m in diameter. Deep erosion of the landslide toe in subsequent years indicates, however, that all sizes were transportable by the available flows. Cobbles and coarse pebbles were the predominant sediments initially covering the downstream limb of the wave; finer gravel and sand covered most of the channel downstream of the wave.

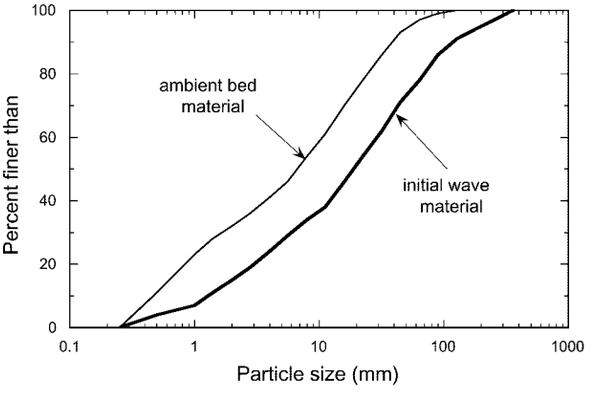

Figure 8. Particle-size distributions of subsurface bulk samples of ambient bed material and of initially deposited landslide material collected 50 m downstream of the landslide in summer 1995.

For modeling purposes, we used the average particle-size distribution of subsurface material sampled in 1995 from four pits at 200–400 m to represent the initially deposited sediment-wave material; we used the average distribution sampled in 1995 from three pits downstream of the leading edge of the wave (1000–1200 m) to represent ambient bed material. The initially deposited wave material was coarser than but sorted similarly to (D_{50} = 19.0 mm, where D_i equals the particle size finer than cumulative percentage i; σ_ϕ = 2.5, where σ_ϕ equals the standard deviation of the particle-size distribution [phi scale]) ambient bed material (D_{50} = 6.7 mm; σ_ϕ = 2.4) (Fig. 8).

In order to investigate longitudinal variations in bed texture, we computed D_{16}, D_{50}, and D_{84} from surface particle-size distributions that were averaged over >50-m-long channel segments in the downstream limb (Fig. 9). For each 50 m segment, averages were calculated by weighting individual pebble counts by patch area. Downstream fining in surface particles is evident as decreases in D_{50} and D_{84} down to 700–1000 m, approximately where the wave merges texturally as well as topographically with the ambient channel (Fig. 5). With time, the bed surface became coarser not only over new sections inundated by the advancing wave in 1996 and 1997, but also over the original extent of the downstream limb (620 m), as finer material was selectively transported from the supply-limited reach downstream of the bed-load trap created by the lake. Parallel variations in subsurface size indicated that bed armoring was pervasive but weak; the ratio of local values of surface D_{50} to subsurface D_{50} was generally <2. A slight depression in surface D_{84} and D_{50} at ~450 m between 1996 and 1997 was created by rounded pebbles that were transported through the lake and over the remnants of the landslide dam and deposited among the reworked landslide material during WY 1997. Slight increases in particle size were evident as far downstream as 1500 m in 1997, and we found characteristic landslide cobbles as far as 1800 m. An increase in rounded pebbles over the downstream limb was evident from pebble-count data at cross sections in later years (Fig. 9). Finally, channel topography forced local fining of the bed surface, specifically at the distal end of a large pool and point bar (~700 m) and at the upstream end of a long pool (~1600 m) (Fig. 4). Pools centered at 1100 m and 1400 m did not show such a dip because they were flanked by large coarse bars.

ABRASION RATES

Rapid downstream fining and net loss of landslide material was partly a result of particle abrasion. Our abrasion-mill experiment of 100 m runs with cumulative travel distances up to 1000 m showed a decrease in the Sternberg abrasion coefficient (Sternberg, 1875; Kodama, 1991; α_w in $M_x/M_0 = e^{-\alpha_w X}$, where M_x = mass of bed-load particles after travel distance X; M_0 = mass of bed-load particles at the starting point) from α_w = 1.0 km^{-1} at 100 m to α_w = 0.46 km^{-1} at 1000 m (Fig. 10). The variation of α_w with travel distance

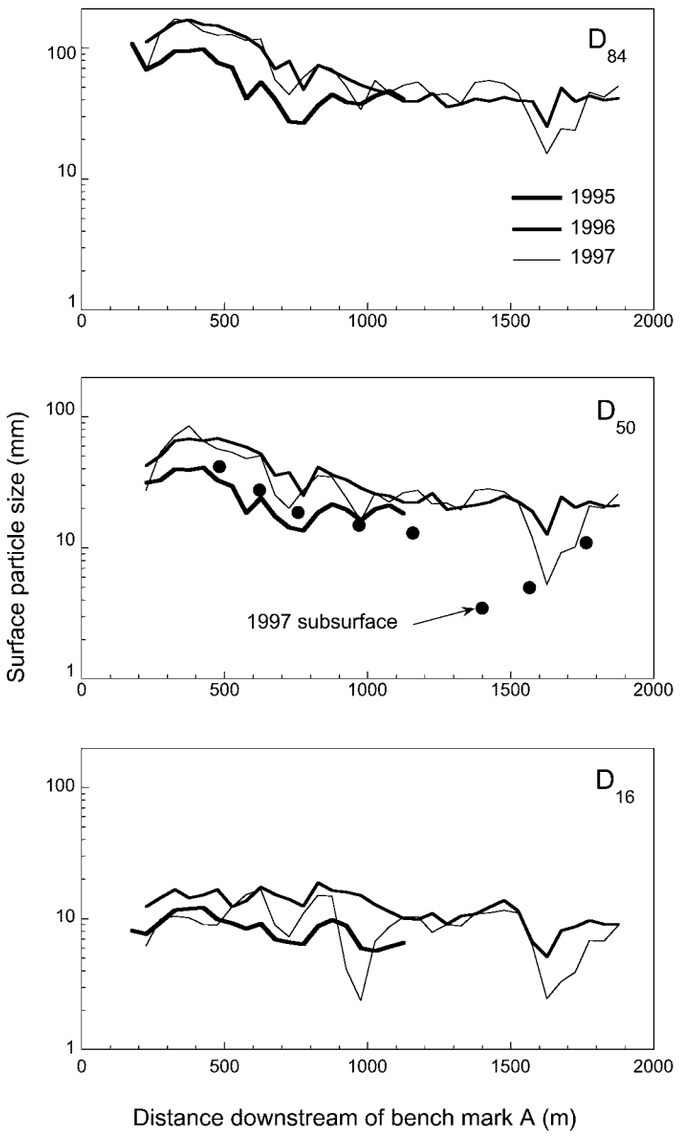

Figure 9. Longitudinal variation in particle sizes D_{16}, D_{50}, and D_{84} of surface bed material averaged over 50-m-long segments of the downstream limb of the wave in 1995, 1996, and 1997; and subsurface D_{50} measured in 1997.

fits a power relation well ($\alpha_w = 4.92x^{-0.344}$; $r^2 = 1.00$). Shorter runs of 25 m using initially deposited wave material yielded values of α_w as high as 3 km^{-1}. In contrast, ambient gravel showed little variation in α_w with travel distance, and the α_w value (0.13 km^{-1}) remained lower than α_w values of initially deposited wave material at the distal end of the evident wave (1000 m). Initially, high abrasion rates were likely caused by rapid wearing of the sharp edges and weathering rinds of regolith particles. These trends suggest that the wave material will continue to wear faster than ambient gravel as it travels beyond the study reach.

To our knowledge, the values of α_w for wave material are the highest reported. Although this material is obviously weak, the high values of α_w may be partly due to our abrasion mill. The mean abrasion rate of the ambient gravel ($\alpha_w = 0.13$ km^{-1}), which consists predominantly of graywacke and shale, provides a comparison with previously measured values of α_w. Maximum values for graywacke are 0.0039 km^{-1} (Shaw and Kellerhals, 1982) and 0.27 km^{-1} for shale (Gies and Gellner, 1982). We conclude that our estimates of abrasion rates may be high relative to other laboratory-determined rates, but by no more than an order of magnitude.

LONGITUDINAL VARIATION IN BED-MATERIAL TRANSPORT

The sediment wave represents a disturbance in sediment transport throughout the affected reach. To examine this disturbance, we analyzed longitudinal variations in sediment transport for the first 2 yr after the landslide, assuming that our study reach included the entire affected reach. Trapping of bed load behind the landslide dam from 1995 to 1997 created a zero-transport datum from which to compute longitudinal variations in annual sediment flux. Annual bulk volume of bed material transported from each 20 m section of channel to the next was computed from sediment continuity, $O = I + \Delta S - A$, where O = output, I = input, ΔS = change in storage, and A = loss of bed load to abrasion.

Starting from the zero datum at the dam ($I = 0$), the output from one section is the input for the next section downstream. The fraction of the bed-load output that is abraded to suspended load is computed from the local abrasion coefficient downstream of the dam (Fig. 10). We assume that the abrasion rate downstream of 1000 m equals that of the ambient gravel because scour and fill of the bed in this reach involves mostly ambient material. We only examined longitudinal variations downstream of the dam because of the lack of resolution created by the wide spacing of surveys upstream of the dam. However, we used the cross sections upstream of the dam to estimate ambient total bed material yield for WY 1997. This estimate represents a maximum because it includes fine material that would not have been deposited in the bed without the backwater effect of the dam. In this period, nearly all material transported downstream of the dam originated from the landslide toe or the bed. Little of the fine sediment that passed through the pond was deposited on the downstream limb of the sediment wave; thus this contribution can be disregarded.

In WY 1996 and WY 1997, bed material transport increased downstream of the dam, peaked, and then declined, whereas transport rates of suspended sediment derived from abrasion of bed-load particles (not including sediment transported through the pond) increased steadily downstream, surpassing bed-load transport rates in WY 1997 (Fig. 11). Peak rates were similar but shifted downstream from 400 m to 800 m in the later year.

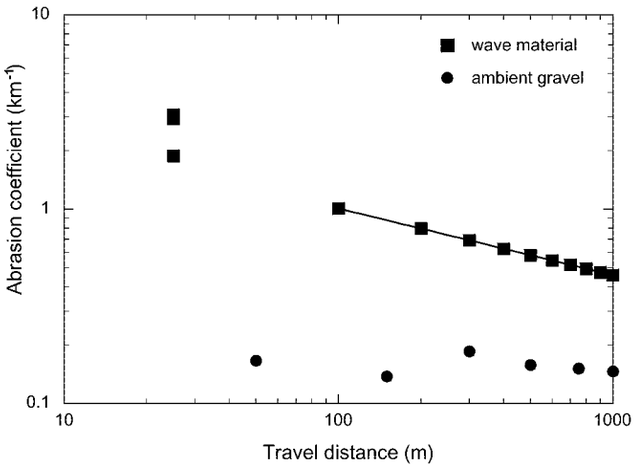

Figure 10. Variation of particle-abrasion rate with transport distance measured in an abrasion mill.

The downstream decrease in bed-material transport was caused by deposition behind the leading edge of the wave, as well as abrasion of bed material and conversion to suspended sediment. In WY 1997, transport rates recovered farther downstream, perhaps manifesting oscillatory scour-and-fill behavior. In both years, the end of the surveyed reach was beyond any observable expressions of the wave.

The merging of local particle size and gradient with ambient conditions at the leading edge of the wave, as well as a lack of change in bed topography, indicates the point of reestablishment of bed-load transporting conditions uninfluenced by the wave. Therefore, calculated transport rates at the end of the study reach should approximate those associated with ambient conditions in the channel, if it is assumed that we were truly beyond the influence of the wave. The farthest-downstream transport rate for WY 1997 (5800 $m^3 \cdot yr^{-1}$) was half of that estimated by the rate of channel filling in the upstream limb (11 700 $m^3 \cdot yr^{-1}$), which should approximate the ambient bed-material load of the river for that year. However, as we have previously suggested in this paper, this discrepancy may be due to the pond trapping material that would otherwise have been suspended and transported downstream. Nevertheless, transport rates at the end of the wave were lower in WY 1997 than in WY 1996, despite the higher discharges in WY 1997. Surface particle size remained nearly constant between 1996 and 1997 (Fig. 9), whereas gradient decreased (Fig. 5). This change may have locally decreased the mobility of upstream parts of the wave and thus may account for the small difference in peak flux rates between the years. However, according to our assumption, ambient transport conditions would have to gradually be reestablished at some point downstream. Apparently, the resolution of our data was not sufficient to recreate this.

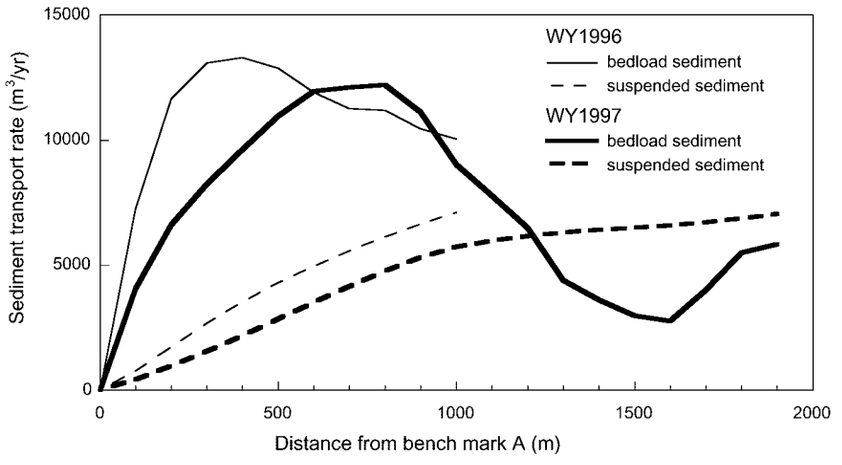

Figure 11. Longitudinal variation in annual transport rates of bed-load and suspended sediment in the downstream limb of the sediment wave.

Changes in the wave profile can be explained with a simple model. The wave causes a discontinuity in particle transport and disequilibrium longitudinally in transport rate, but at some point downstream of the wave, ambient transport capacity is satisfied by erosion of the bed upstream. At this point, the channel is adjusted as it was upstream of the wave to an equal sediment load before the wave was formed. If the wave were composed of immobile material, ambient transport capacity would be satisfied by scour of the bed starting downstream of the wave front (Fig. 12A). If the wave material was more mobile, more of the transport capacity would be satisfied by scour of the wave and less by scour of the bed downstream (Fig. 12B). If just enough of the wave were scoured to satisfy capacity, the wave would appear to decay in place with no change in the bed downstream (Fig. 12C). Finally, if erosion of the wave more than satisfied capacity, deposition would occur downstream of the wave and the wave front would advance (Fig. 12D). Evolving wave profiles and corresponding longitudinal patterns of bed-material transport can be used to categorize wave behavior. Case C (of Fig. 12) fits the evolutionary stage of the wave in WY 1996; case D (of Fig. 12) fits that of WY 1997 (Figs. 5 and 11).

MODEL PREDICTIONS

We used a one-dimensional model designed for routing sediment pulses in heterogeneous, armored, gravel-bed channels to reconstruct the 1995–1999 evolution of the wave and thereby add a theoretical basis for our observations. The model is described elsewhere (Cui et al., 2002b) and is briefly summarized next. The model allows for fining downstream as a function of selective transport and attrition. The model incorporates the St. Venant shallow-water equations for water continuity and momentum with four governing equations describing channel-bed evolution: (1) a form of the Exner equation for mass conservation of heterogeneous sediment, (2) a transfer function to regulate the exchange of particle sizes between surface and subsurface layers of the bed (Toro-Escobar, 1995), (3) a bed-load transport function (the surface-based bed-load transport function of Parker [1990a, 1990b]), and (4) the Keulegan resistance relationship.

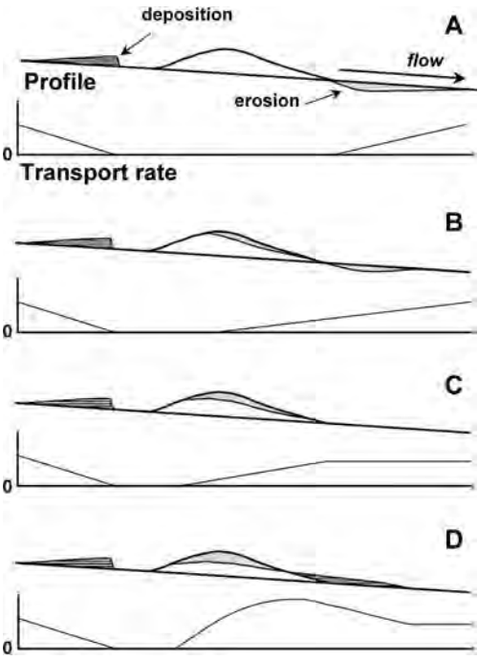

Figure 12. Evolution of idealized dispersive waves and associated longitudinal variations in sediment transport. Cases: (A) Nonerosive wave. (B) Partially erosive wave. (C) Stationary wave. (D) Advancing wave. Abrasion of wave material and conversion to suspended sediment are neglected.

TABLE 1. VALUES OF INPUT PARAMETERS USED IN MODEL PREDICTIONS OF WAVE EVOLUTION

Initial channel characteristics	Value
Original channel slope	0.00128 m/m
Channel width	44 m
Sediment porosity	0.43
Active-layer thickness (L_w)	0.8 m
Reach length	4.35 km
Particle-size distribution of ambient bed material	D_{50} = 5.1 mm; σ_ϕ = 2.4
Average abrasion coefficient of ambient bed material	0.1
Wave characteristics	**Value**
Average abrasion coefficient of initial wave material	0.3
Particle-size distribution of initial wave material	D_{50} = 15 mm; σ_ϕ = 2.5
Input location	2.5–3.35 km

To employ the model, we made some simplifying assumptions: (1) Nonuniformities in channel width, slope, and particle size before the landslide were too small to significantly affect the evolution of the sediment wave. (2) There were no significant tributary inputs of sediment or water. (3) Only gravel ($D > 2$ mm) is included as part of the wave. Abrasion products are lost to suspension.

Channel-specific data sets required as input to the model (Table 1) are as follows: (1) Predisturbance channel characteristics included transversely averaged mean bed elevations at channel distances, channel width, active layer thickness, reach length, bed porosity, ambient abrasion coefficient, and particle-size distributions of surface and subsurface sediments. (2) Initial sediment-wave characteristics comprised transversely averaged mean bed elevations at channel distances, abrasion coefficient, and particle-size distributions of sediment input. (3) Discharge records provided the mean daily discharge from the downstream gauging station adjusted for drainage area.

In addition, the user specifies total calculation time, time increment for calculations, the number of nodes, and the increment length over which to calculate. Inputs to the model are detailed in Hansler (1999).

MODEL RESULTS

The numerical model reproduces the general forms of evolutionary stages of the mean-elevation profile reasonably well (Fig. 13). The modeled profile of the first year (1995) is a simplification of the sediment wave superposed on the model-generated initial profile. Already there are bar-scale discrepancies owing to local topographic forcing that persist in later years. The model also overpredicts deposition upstream of the landslide because of apparently inflated estimates of ambient bedload transport. The model performs best downstream of the landslide, where general agreement is excellent for every year. The salient feature of modeled wave evolution is that, in agreement with topographic data, peak aggradation remains at the initial entry point of the landslide; thus the wave does not translate. An analysis of the sensitivity of results to uncertainties in input parameters is reported elsewhere (Cui et al., 2002b). Predictions are robust for reasonable ranges of input parameters, and none show significant departures from the general characterizations of predicted wave evolution described herein for the Navarro River sediment wave.

DISCUSSION AND CONCLUSIONS

A large landslide entering a gravel-bed river at the close of the annual high-runoff season offered a rare opportunity to observe the evolution of a sediment wave from initial to final stages. This case was relatively simple and offered a test of the relative tendencies of translation and dispersion of sediment waves in heterogeneous, gravel-bed channels with bar-pool topography. The details of the case are as follows:

1. The wave entered the channel in a single event, and other than bed load carried into the reach from upstream, there were no significant additional inputs to the study reach.

2. The preexisting channel was relatively uniform. The channel was single-thread and, other than a single bend, was only slightly sinuous. The only significant variations in width, depth, slope, or particle size were associated with bar-pool morphology.

3. Resistant banks restricted channel response to changes within the original boundaries of the active channel.

4. Flow events in years after the landslide, some exceeding bankfull levels, were high enough to mobilize all particle sizes introduced by the landslide.

In the simplest case, the sediment input would have the same particle-size distribution as the ambient bed material. In the Navarro River case, the input material had a wider distribution and a larger median size than ambient bed material. Wide grading of input material would have promoted selective transport and thereby enhanced wave dispersion. However, the coarseness of the landslide deposit did not prevent deep channel incision to nearly the original bed elevation. Moreover, such differences in particle size between input and ambient probably characterize many large sediment inputs.

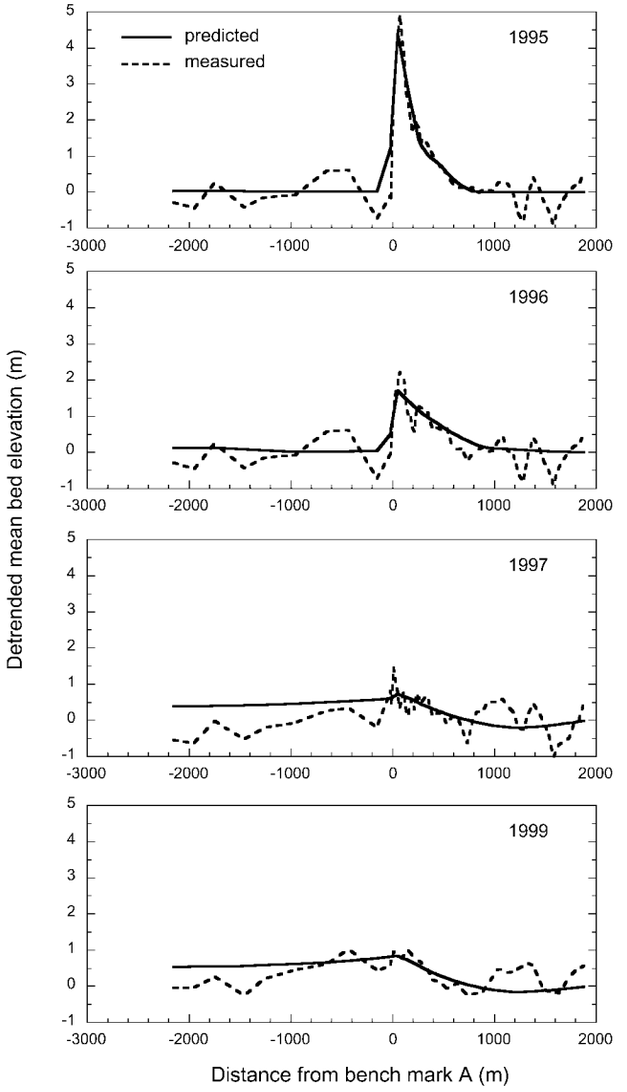

Figure 13. Comparisons between measured detrended mean bed elevations (mean gradient removed) and bed elevations predicted by the numerical model. The modeled profile for 1995 is the input wave form and thus is not a prediction.

Given the simplicity of these natural conditions, accurate reconstructing of the evolution of longitudinal patterns of mean bed elevation by a physically based, numerical model that incorporates interactions between unsteady flow, bed topography, and transport of heterogeneous bed load affirms the main conclusion drawn from field observations. The tendency for dispersion of sediment waves in natural gravel-bed channels is apparently so strong that translation is undetectable, barring some special conditions such as those described next.

The downstream shift in peak bed-load flux in the downstream limb of the wave from WY 1996 to WY 1997 did, however, manifest translatory behavior of a property of the wave, albeit an outcome of purely dispersive redistribution of bed material. In waves where topographic data are insufficient to accurately identify wave behavior, a more apparent translation of bed-load transport rates could give the impression of the dominance of translation. Moreover, longitudinal variations in bed mobility may have as much or greater significance to lotic ecosystems as variations in bed elevation or texture.

Tendencies for significant wave translations may lie outside characteristic fluvial conditions for gravel-bed channels. At one extreme, low Froude numbers, which are more typical of sand-bed channels, can promote wave translation, as can fine-grained wave material in gravel-bed channels (Cui et al., 2002b; Lisle et al., 2001). At the other extreme, debris flows, torrents or bed-load flows in steep, bouldery channels commonly form a pronounced, rapidly translating front of coarse material and woody debris that is followed by more erodible, finer-grained material (Innes, 1983; Costa, 1984; Iseya et al., 1990).

Greater channel nonuniformity than that expressed in this relatively simple case may favor even greater rates of dispersion. In general, greater nonuniformity would create greater spatial variation in tractive forces. This likelihood would tend to promote greater transverse and longitudinal variations in bed-load transport and cause particles in high-transport zones to race forward as others deposited in peripheral zones are left behind. The agreement between a one-dimensional model and a full-dimensional field case in this study suggests that dispersion would have also dominated in a still simpler channel. However, certain downstream patterns in transport capacity at the reach scale may force downstream-propagating sequences of aggradation and degradation that resemble translation of a sediment wave. More specifically, a river could fill and scour in a downstream pattern as a spreading wave advanced into a sequence of sedimentation zones. Such large-scale variations in alluviation are well known (Church, 1983; Grant et al., 1990), but system-scale interactions with sediment fluxes are poorly understood. Recognition of the dispersive behavior of sediment waves in gravel-bed rivers may simplify sediment routing strategies, but greater understanding of sediment routing in natural systems will require greater understanding of sediment movement over spatial scales longer than those of individual sediment waves such as the one reported here.

The dominance of dispersion in the evolution of sediment waves in gravel-bed rivers has important implications for the management of lotic ecosystems. In the absence of translation of sediment waves, downstream sedimentation tends to be pervasive rather than punctuated. Dispersion and overlapping of sediment waves from a number of sources and their interaction with large-scale channel topography can make it difficult to attribute an observed sediment effect to its source. One of the perceived drawbacks of the decommissioning of dams is that the potentially large volumes of released sediment may cause large impacts downstream. However, among all the scenarios of the fate of such sediment releases, the one assuming maximum dispersion predicts the least magnitude of impact at any

point downstream. Such general predictions may motivate applications of more comprehensive models to predict sediment routing and channel response.

ACKNOWLEDGMENTS

Yantao Cui provided the numerical model and guided us in running it. Thembi Borras, Bryan Dussell, Gwen Erickson, Sam Flanagan, Sherman Garinger, Lex Rohn, Bonnie Smith, Stephen Tordoff, and Giovanni Vadurro provided assistance in field work. The Lousiana-Pacific Corporation and Mendocino Redwoods Corporation provided logistical support and access to the field site. Sam Flanagan, Alejandro Ramirez, and Lizzy Gilliam helped conduct abrasion experiments. We gratefully acknowledge their assistance. Insightful reviews by Mike Church, Peter Knuepfer, and Dave Montgomery helped to improve the paper.

REFERENCES CITED

Benda, L., and Dunne, T., 1997, Stochastic forcing of sediment routing and storage in channel networks: Water Resources Research, v. 33, p. 2865–2880.

Buffington, J.M., and Montgomery, D.R., 1999, A procedure for classifying textural facies in gravel-bed rivers: Water Resources Research, v. 35, p. 1903–1914.

Church, M., 1983, Pattern of instability in a wandering gravel bed channel, *in* Collinson, J.D., and Lewin, J., eds., Modern and ancient fluvial systems: Oxford, Blackwell Scientific Publications, p. 169–180.

Church, M., McLean, D.G., and Wolcott, J.F., 1987, River bed gravels: Sampling and analysis, *in* Bathurst, J.C., Thorne, C.R., and Hey, R.D., eds., Sediment transport in gravel-bed rivers: Chichester, John Wiley and Sons, p. 43–88.

Costa, J.E., 1984, Physical geomorphology of debris flows, *in* Costa, J.E., and Fleischer, P.J., eds., Developments and applications or geomorphology: New York, Springer-Verlag, p. 268–317.

Cui, Y., Parker, G., Lisle, T.E., Gott, J., Hansler, M.E., Pizzuto, J.E., Almendinger, N.E., and Reed, J.M., 2002a, Sediment pulses in mountain rivers: Part 1. Experiments: Water Resources Research (in press).

Cui, Y., Parker, G., Pizzuto, J.E., and Lisle, T.E., 2002b, Sediment pulses in mountain rivers: Part 2. Comparison between experiments and numerical predictions: Water Resources Research (in press).

Dodd, A.M., 1998, Modeling the movement of sediment waves in a channel [M.S. thesis]: Arcata, California, Humboldt State University, 53 p.

Gies, R., and Geller, F.J., 1982, Pressure gradients and degradation at the hydrotransport of coarse washery wastes, *in* Eighth International Conference on the Hydraulic Transport of Solids in Pipes: Johannesburg: Cranfield, England, BHRA Fluid Engineering, p. 227–240.

Gilbert, G.K., 1917, Hydraulic mining debris in the Sierra Nevada: U.S. Geological Survey Professional Paper 105, 154 p.

Grant, G.E., Swanson, F.J., and Wolman, M.G., 1990, Pattern and origin of stepped-bed morphology in high-gradient streams, western Cascades, Oregon: Geological Society of America Bulletin, v. 102, p. 340–352.

Hansler, M.E., 1999, Sediment wave evolution and analysis of a one-dimensional sediment routing model, Navarro River, northwestern California [M.S. thesis]: Arcata, California, Humboldt State University, 128 p.

Innes, J.L., 1983, Debris flows: Progress in Physical Geography, v. *7*, p. 467–501.

Iseya, F., Ikeda, H., Maita, H., and Kodama, Y., 1990, Fluvial deposits in a torrential gravel-bed stream by extreme sediment supply: Sedimentary structure and depositional mechanism, *in* Third International Workshop on Gravel-bed Rivers: Firenza, Italy: Cichester, England, John Wiley and Sons, 24 p.

Kodama, Y., 1991, Effect of abrasion on downstream gravel-size reduction in the Watarse River, Japan: Field work and laboratory experiment [Ph. D. dissertation]: Tsukuba, Japan, University of Tsukuba, 155 p.

Knighton, A.D., 1989, River adjustments to changes in sediment load: The effects of tin mining on the Ringarooma River, Tasmania, 1875–1984: Earth Surface Processes and Landforms, v. 14, p. 333–359.

Lisle, T.E., and Madej, M.A., 1992, Spatial variation in armouring in a channel with high sediment supply, *in* Billi, P., Hey, R.D., Thorne, C.R., and Tacconi, P., eds., Dynamics of gravel-bed rivers: Chichester, John Wiley and Sons, p. 277–291.

Lisle, T.E., Pizzuto, J.E., Ikeda, H., Iseya, F., and Kodama, Y., 1997, Evolution of a sediment wave in an experimental channel: Water Resources Research, v. 33, p. 1971–1981.

Lisle, T.E., Cui, Y., Parker, G., Pizzuto, J.E., and Dodd, A.M., 2001, The dominance of dispersion in the evolution of bed material waves in gravel bed rivers: Earth Surface Processes and Landforms, v. 26, p. 1409–1420.

Madej, M.A., and Ozaki, V., 1996, Channel response to sediment wave propagation and movement, Redwood Creek, California, USA: Earth Surface Processes and Landforms, v. 21, p. 911–927.

Manson, M.W., 1984, Geology and geomorphic features relating to landsliding, Navarro southeast (Cold Spring) 7.5 minute quadrangle, Mendocino County, California: Sacramento, California Department of Conservation, Division of Mines and Geology, scale 1:24 000.

Meade, R.H., 1985, Wavelike movement of bedload sediment, East Fork River, Wyoming: Environmental Geology and Water Science, v. 7, p. 215–225.

Miller, D.J., and Benda, L.E., 2000, Effects of punctuated sediment supply on valley-floor landforms and sediment transport: Geological Society of America Bulletin, v. 112, p. 1814–1824.

Mosley, M.P., and Tindale, D.S., 1985, Sediment variability and bed material sampling in gravel-bed rivers: Earth Surface Processes and Landforms, v. 10, p. 465–482.

Parker, G., 1990a, Surface-based bedload transport relation for gravel rivers: Journal of Hydraulic Research, v. 28, p. 417–436.

Parker, G., 1990b, The ACRONYM series of PASCAL programs for computing bedload transport in gravel rivers: Minneapolis, University of Minnesota, St. Anthony Falls Laboratory, External Memorandum M-220, 124 p.

Pitlick, J., 1993, Response and recovery of a subalpine stream following a catastrophic flood: Geological Society of America Bulletin, v. 105, p. 657–670.

Roberts, R.G., and Church, M., 1986, The sediment budget in severely disturbed watersheds, Queen Charlotte Ranges, British Columbia: Canadian Journal of Forestry Research, v. 16, p. 1092–1106.

Shaw, J., and Kellerhals, R., 1982, The composition of recent alluvial gravels in Alberta river beds: Alberta Research Council Bulletin, v. 41, 151 p.

Sowma-Bawcom, J.A., 1996, Breached landslide dam on the Navarro River, Mendocino County, California: California Geology, Sept.–Oct., p. 120–127.

Sutherland, D.G., Hansler, M.E., Hilton, S.J., and Lisle, T.E., 1998, Sediment wave evolution and channel morphologic changes resulting from a landslide, Navarro River, northwestern California: Geological Society of America Abstracts with Programs, v. 30, no. 7, p. A-360.

Sternberg, H., 1875, Untersuchungen Uber Langen und Querprofil geschiebefuhrender Flusse: Berlin, Zeitschrift für Bauwesen, v. 25 p. 483–506.

Toro-Escobar, C.M., 1995, Differential transport and deposition of gravel-sand mixtures in an aggrading river, [M.S. thesis]: Minneapolis, University of Minnesota, 121 p.

Turner, T.R., 1995, Geomorphic response of the Madison River to point sediment loading at the Madison Slide, southwest Montana [M.S. thesis]: Bozeman, Montana State University, 98 p.

Wolman, M.G., 1954, A method of sampling coarse river bed material: Transactions, American Geophysical Union, v. 35, p. 951–956.

MANUSCRIPT RECEIVED BY THE SOCIETY JUNE 14, 2001
REVISED MANUSCRIPT RECEIVED MARCH 14, 2002
MANUSCRIPT ACCEPTED MARCH 21, 2002

Printed in the USA